Title

Multiple roles of heterogeneous nuclear ribonucleoprotein K during skeletal muscle cell differentiation

Authors

Keisuke Hitachi[1], Yuri Kiyofuji[1], Masashi Nakatani[2], and Kunihiro Tsuchida[1,*]

Affiliations

[1]Division for Therapies against Intractable Diseases, Institute for Comprehensive Medical Science (ICMS), Fujita Health University, Toyoake, Japan, [2]Faculty of Rehabilitation and Care, Seijoh University, Tokai, Japan

*Correspondence: tsuchida@fujita-hu.ac.jp

Abstract

RNA-binding proteins (RBPs) regulate cell physiology via the formation of ribonucleic-protein complexes with coding and non-coding RNAs. RBPs have multiple functions in the same cells; however, the precise mechanism through which their pleiotropic functions are determined remains unknown. In this study, we revealed the multiple inhibitory functions of hnRNPK for myogenic differentiation. We first identified hnRNPK as a lncRNA *Myoparr* binding protein. Gain- and loss-of-function experiments showed that hnRNPK repressed the expression of *myogenin* at the transcriptional level via binding to *Myoparr*. Moreover, hnRNPK repressed the

expression of a set of genes coding for aminoacyl-tRNA synthetases in a *Myoparr*-independent manner. Mechanistically, hnRNPK regulated the eIF2α/Atf4 pathway, one branch of the intrinsic pathways of the endoplasmic reticulum sensors, in differentiating myoblasts. Thus, our findings demonstrate that hnRNPK plays multiple lncRNA-dependent and -independent roles in the inhibition of myogenic differentiation, indicating that the analysis of lncRNA-binding proteins will be useful for elucidating both the physiological functions of lncRNAs and the multiple functions of RBPs.

Keywords

transcriptional regulation, myogenic differentiation, RNA-binding protein, endoplasmic reticulum stress

Introduction

Long non-coding RNAs (lncRNAs), which are >200 nucleotides (nt) in length and which do not encode more than 100 amino acids, are emerging as important regulators in diverse biological processes, including transcription, splicing, RNA stability, and translation (Statello et al., 2021). LncRNAs are pervasively transcribed from the noncoding genomic DNA; cis-regulatory regions, including promoter and enhancer, introns, 3' untranslated regions, and repetitive sequences (Chakraborty et al., 2014). LncRNAs are also expressed from the antisense direction of the coding genomic DNA (Hon et al., 2017). Thus, most of the genomic regions have the potential to express lncRNAs. Thus far, more than 260,000 lncRNA genes are registered in the LncBook, which is a curated knowledge-based database for human lncRNAs (Ma et al., 2019). Since lncRNAs exert their molecular functions by interacting with proteins (Hitachi and Tsuchida, 2020), their molecular functions differ widely, depending on the interacting partners.

As lncRNA-interacting factors, RNA-binding proteins (RBPs) are essential to determine the molecular function of each lncRNA (Statello et al., 2021). In the human genome, more than 1,500 genes encode RBPs (Gerstberger et al., 2014). RBPs consist of ribonucleoprotein complexes together with lncRNAs to regulate various biological aspects. For example, the association of Ddx5/Ddx17 with lncRNAs, such as *SRA*, *mrhl*, *MeXis*, or *Myoparr*, is required to activate the expression of downstream genes (Caretti et al., 2006; Hitachi et al., 2019; Kataruka et al., 2017; Sallam et al., 2018). RBPs, including NONO, SFPQ, FUS, and RBM14, associate with *Neat1*, which is a highly abundant lncRNA in mammals, to form a large membrane-less structure paraspeckle in the nucleus (Hirose et al., 2019). A ubiquitously expressed RBP, known as human

antigen R (HuR) associates with lncRNAs and regulates their stability; HuR increases the cytosolic *linc-MD1* levels in skeletal muscle cells (Legnini et al., 2014), whereas it promotes the decay of *lincRNA-p21* in HeLa cells (Yoon et al., 2012). Additionally, RBPs are also involved in RNA splicing, polyadenylation, RNA transport, and translation (Kelaini et al., 2021). The majority of RBPs are involved in multiple biological processes in concert with lncRNAs (Briata and Gherzi, 2020; Jonas et al., 2020; Nostrand et al., 2020), and mutations in genes coding for RBPs are associated with human genetic disorders (Gebauer et al., 2021).

Heterogeneous nuclear ribonucleoprotein K (hnRNPK), a member of the heterogeneous nuclear ribonucleoprotein family, has multiple roles, including chromatin remodeling, transcription, RNA splicing, and translation (Bomsztyk et al., 2004; Wang et al., 2020). hnRNPK acts together with *lincRNA-p21*, *EWSAT1*, and *lncRNA-OG*, to regulate the expression of downstream genes in mouse embryonic fibroblasts, Ewing sarcoma, and bone marrow-derived mesenchymal stem cells (Dimitrova et al., 2014; Howarth et al., 2014; Tang et al., 2018). However, the molecular function of hnRNPK in skeletal muscle cells has not been fully elucidated. LncRNA *Myoparr* is an essential regulator of skeletal muscle cell proliferation and differentiation (Hitachi et al., 2019). We previously identified hnRNPK as a candidate for *Myoparr*-associated protein in skeletal muscle cells (Hitachi et al., 2019), suggesting the unique functions of *Myoparr*-associated hnRNPK during myogenic differentiation. In the present study, we revealed the inhibitory role of hnRNPK as a *Myoparr*-associated protein in skeletal muscle cell differentiation. Moreover, by comparing the downstream genes regulated by *Myoparr* and hnRNPK, we also found a *Myoparr*-independent role of hnRNPK during myogenic differentiation. Our findings reveal that hnRNPK plays multiple

lncRNA-dependent and -independent roles in skeletal muscle cell differentiation and will contribute to elucidating the complex roles of RBPs in cell differentiation.

Materials and Methods

Cell cultures, siRNA transfection, and ISRIB treatment

A mouse myoblast cell line, C2C12, was cultured in Dulbecco's modified Eagle medium (DMEM) supplemented with 10% fetal bovine serum at 37°C under 5% CO_2. Myogenic differentiation was induced by replacing the medium with the differentiation medium, DMEM supplemented with 2% horse serum. C2C12 myoblasts were transfected with 50 nM of Stealth RNAi (Thermo Fisher Scientific, Waltham, MA, USA) using Lipofectamine 3000 (Thermo Fisher Scientific) according to the manufacturer's protocol. The following siRNAs were used: Stealth RNAi siRNA negative control (Negative Control, Med GC, Thermo Fisher Scientific), stealth RNAi for *Myoparr*, and stealth RNAi siRNAs specific for *hnRNPK* (MSS205172 and MSS205173, Thermo Fisher Scientific). The siRNA sequences are listed in Supplemental Table 1. At 24 h after siRNA transfection, myogenic differentiation was induced. At 24 h or 72 h after differentiation induction, cells were collected for the analysis of RNAs and proteins. For ISRIB treatment, the differentiation medium was added either with or without 1 μM ISRIB (Cayman Chemical Company, Ann Arbor, MI, USA).

RNA isolation, reverse transcription reaction, and quantitative RT-PCR

Total RNA was extracted from C2C12 cells using ISOGEN II reagent (Nippon Gene, Tokyo, Japan) according to the manufacturer's protocol. After DNase I

(Thermo Fisher Scientific) treatment, total RNA was used for reverse transcription reaction using SuperScript III Reverse Transcriptase (Thermo Fisher Scientific) or ProtoScript II Reverse Transcriptase (New England Biolabs (NEB), Beverly, MA, USA) with random or oligo (dT) primers (Thermo Fisher Scientific). Quantitative real-time PCR was conducted using SYBR Premix Ex Taq (Takara Bio Inc., Shiga, Japan) and a Thermal Cycler Dice Real Time System TP800 (Takara Bio Inc.). The results were normalized to the *Rpl26* expression. The primers used are listed in Supplementary Table 1.

Protein extraction and Western blotting

Cells were lysed in RIPA buffer (50 mM Tris-HCl (pH 8.0), 150 mM NaCl, 0.1% SDS, 1% Triton X-100, 0.5% sodium deoxycholate) containing protease inhibitors (1 mM phenylmethylsulfonyl fluoride, 1 μg/ml aprotinin, 4 μg/ml leupeptin) and phosphatase inhibitors (5 mM NaF, 5 mM β-glycerophosphate, 1 mM Na_3VO_4). The protein concentration was measured using a Pierce BCA Protein Assay Kit (Thermo Fischer Scientific). Equal amounts of protein were used for Western blotting. The following primary antibodies were used: myogenin antibody (F5D) (sc-12732, Santa Cruz Biotechnology, Dallas, TX, USA), MHC antibody (MF20, Developmental Studies Hybridoma Bank (DSHB)), hnRNPK antibody (#4675, Cell Signaling Technology (CST), Beverly, MA, USA), TIAR antibody (#8509, CST), and Atf4 antibody (693901, BioLegend, San Diego, CA, USA). The following HRP-linked secondary antibodies were used: anti-mouse IgG (#7076, CST) and anti-rabbit IgG (#7074, CST). Can Get Signal Immunoreaction Enhancer Solution (Toyobo, Osaka, Japan) was used when necessary. The signal was detected with ImmunoStar LD reagent (FUJIFILM Wako,

Osaka, Japan) using a cooled CCD camera system (Light-Capture, ATTO, Tokyo, Japan).

Immunofluorescence assay

Immunofluorescence analyses of C2C12 cells were performed as previously described (Hitachi et al., 2019). Briefly, 24 h or 72 h after the induction of differentiation, cells were fixed with 4% PFA and permeabilized with 0.2% Triton X-100. After blocking with 5% FBS, cells were stained with an anti-myogenin antibody (F5D, DSHB) or with an anti-MHC antibody (MF20, DSHB). Nuclei were counterstained with DAPI (Dojindo, Kumamoto, Japan). A DMI4000B microscope with a DFC350FX CCD camera (Leica, Wetzlar, Germany) was used for visualization of signals. Images were analyzed using the Image J software program (ver. 1.49).

Identification of *Myoparr*-binding proteins

Myoparr-binding proteins were collected with the RiboTrap Kit (Medical & Biological Laboratories (MBL), Aichi, Japan) using BrU labeled RNAs, as described previously (Hitachi et al., 2019). BrU-labeled *Myoparr* and *EGFP* RNA were prepared using the Riboprobe System (Promega, Madison, WI, USA). The *Myoparr* or *EGFP* RNA (50 pmol) were mixed with the nuclear extract from C2C12 myotubes for 2 h at 4°C. The RNA-protein complexes were collected by Protein G Plus Agarose (Thermo Fisher Scientific) conjugated to an anti-BrdU antibody, and proteins were eluted by adding BrdU. Purified proteins were detected by Western blotting using a specific antibody, as described above.

RNA immunoprecipitation and the RNA pull-down assay

Immunoprecipitation of endogenous RNAs (*Myoparr* or *Xist*) was performed using the RIP-Assay Kit (MBL) using 2×10^7 C2C12 cells, as previously described (Hitachi et al., 2019). The following antibodies were used for RNA immunoprecipitation: normal rabbit IgG (#2729S, CST), anti-HNRNPK pAb (RN019P, MBL), or TIAR mAb (#8509, CST). After treatment with DNase I, immunoprecipitated RNAs was used for the reverse transcription reaction. The precipitation percentage (precipitated RNA vs. input RNA) was calculated by qRT-PCR using the primers listed in Supplementary Table 1.

An RNA pull-down assay was performed with a RiboTrap Kit. Various lengths of *Myoparr* were subcloned into a pGEM-Teasy vector (Promega). BrU-labeled *Myoparr* (10 pmol each) was bound to Protein G Plus Agarose conjugated to an anti-BrdU antibody and mixed with the *in vitro* transcribed/translated hnRNPK protein. After several washing steps, the binding of hnRNPK to *Myoparr* was analyzed by Western blotting using an hnRNPK antibody as described above.

Luciferase reporter assay

The upstream region of *myogenin* (-1650/+51) was PCR-amplified and cloned into the pGL4.20 vector (Promega). The *hnRNPK*-expressing plasmid was a kind gift from Dr. H. Okano (Yano et al., 2005). Proliferating C2C12 cells were transfected with the *myogenin* promoter and *hnRNPK*-expressing plasmid using Lipofectamine 2000 (Thermo Fisher Scientific). The total amount of DNA was kept constant by the addition of the pcDNA3 vector. Cells were collected at 24 h after the induction of differentiation and dissolved in Passive Lysis Buffer (Promega). The effect of hnRNPK on *myogenin*

promoter was measured using a Lumat LB 9507 luminometer (Berthold Technologies, Bad Wildbad, Germany) with the Dual-Luciferase Reporter Assay System (Promega) according to the manufacturer's protocol. The pGL4.74 vector (Promega) was used as an internal control. The relative luciferase activity is shown as the firefly to Renilla luciferase ratio.

To reconstitute the complex chromatin structure and epigenetic regulation *in vitro* (Liu et al., 2001), the upstream regions of *myogenin* (-242/+51 and -1650/+51) were subcloned into the episomal luciferase vector, pREP4-luc, and the -242-Luc and -1650-Luc constructs were generated. To create the -1650Δccawmcc-Luc construct, the upstream region (-971/-902) of *myogenin* was deleted from the -1650-Luc construct. The region containing the putative hnRNPK-binding motif ccawmcc was identified by RBPmap (Paz et al., 2014). The episomal luciferase vector, pREB7-Rluc, was used as an internal control for the luciferase assay. The pREP4-luc and pREP7-Rluc vectors were gifts from Dr. K. Zhao (Liu et al., 2001). Subconfluent C2C12 cells were transfected with the indicated episomal luciferase vectors using Lipofectamine 2000. After myogenic induction, cells were collected and used to measure the relative luciferase activity.

Analysis of downstream genes regulated by *Myoparr* KD and *hnRNPK* KD

Downstream genes regulated by *Myoparr* KD and *hnRNPK* KD were identified as described previously (Hitachi and Tsuchida, 2019) using our RNA-Seq raw data (accession No. DRA005527). Briefly, statistical analysis of differentially expressed genes by *Myoparr* KD and *hnRNPK* KD was performed using DESeq2 ver. 1.12.4 software (Love et al., 2014) with a Wald test (cut-offs: false discovery rate (adjusted

p-value, padj) < 0.05 and log 2 fold change > 0.75 or < -0.75). A pathway analysis of significantly upregulated genes coding for cytosolic aminoacyl-tRNA synthetases was performed based on the KEGG (Kanehisa et al., 2020). A Gene Ontology (GO) analysis of differentially expressed genes was performed with DAVID ver. 6.8 (https://david.ncifcrf.gov/). An enrichment analysis was performed using Metascape (Zhou et al., 2019).

Statistical analysis

Error bars represent standard deviation. Statistical analyses were performed using unpaired two-tailed Student's *t*-tests. For comparisons of more than 2 groups, a one-way ANOVA followed by Tukey's post hoc test was performed using Prism 9 (GraphPad Software, San Diego, CA, USA). Statistical significance is reported in the Figures and Figure legends. *P* values of < 0.05 were considered statistically significant.

Results

Identification of hnRNPK as a *Myoparr*-binding protein in skeletal muscle cells

Our proteomics analysis identified both hnRNPK and TIAR as candidates for *Myoparr*-associated proteins (Hitachi et al., 2019). To reveal whether hnRNPK and TIAR are associated with the *Myoparr* function during myogenic differentiation, we first examined the specific interaction of *Myoparr* with endogenous hnRNPK and TIAR. *In vitro* synthesized *Myoparr* was labeled with 5-bromouridine (BrU) and mixed with the nuclear extract from differentiating C2C12 myoblasts. After purification of *Myoparr* by immunoprecipitation with a BrdU antibody, specific binding between *Myoparr* and hnRNPK protein was confirmed by immunoblotting (Figure 1A). Since binding

between *EGFP* mRNA and hnRNPK was not observed, *EGFP* mRNA was used as a negative control. Intracellular binding between endogenous *Myoparr* and hnRNPK was shown by RNA immunoprecipitation using an hnRNPK-specific antibody without a crosslinking (Figure 1B and C). This enrichment of *Myoparr* by hnRNPK was stronger than that of *Xist*, which interacts with hnRNPK in embryonic stem cells (Chu et al., 2015). Although TIAR protein was retrieved by synthesized *Myoparr*, intracellular endogenous interaction between *Myoparr* and TIAR was not observed (Supplementary Figure 1A-C). These results suggested that hnRNPK cooperatively works with *Myoparr* during skeletal muscle differentiation.

hnRNPK represses the expression of *myogenin* in differentiating myoblasts

During myogenic differentiation, the expression of *Myoparr* gradually increases and is required to activate the expression of *myogenin* (Hitachi et al., 2019). Thus, we examined the changes in the expression of hnRNPK during C2C12 cell differentiation. Although the expression of myogenin was highly increased after myogenic induction, the expression of hnRNPK gradually decreased (Figure 2A), suggesting the regulatory role of hnRNPK in the expression of *myogenin*. We next knocked down *hnRNPK* using the small interfering RNAs (siRNAs) in differentiating C2C12 cells. The knockdown (KD) of *hnRNPK* by two distinct siRNAs was associated with a large increase in the expression of myogenin (Figure 2B). However, an immunocytochemistry analysis of the myogenin expression after *hnRNPK* KD did not show a sufficient increase in the ratio of myogenin-positive cells comparing to the control (Figure 2C). These results indicated that *hnRNPK* KD is not enough to induce the expression of myogenin in cells without the cell-intrinsic expression of myogenin.

We observed that the expression of *myogenin* was significantly increased by *hnRNPK* KD (Figure 2D and E). Although the differences were not statistically significant, the *Myoparr* expression levels also tended to be increased by *hnRNPK* KD (Figure 2F). From these results, we surmise that hnRNPK negatively regulates the expression of *myogenin* at the transcriptional level. The effect of hnRNPK on the transcription of *myogenin* was examined using the *myogenin*-promoter-driven luciferase assay. The overexpression of hnRNPK in differentiating C2C12 cells decreased the *myogenin* promoter activity (Figure 2G), indicating that hnRNPK negatively regulates the expression of *myogenin* via the *myogenin* promoter.

hnRNPK represses the expression of *myogenin* via binding to *Myoparr*

The hnRNPK-binding region of *Myoparr* was determined by RNA pull-down experiments using the various forms of *Myoparr* (Figure 3A). Figure 3B showed that hnRNPK bound to the full-length sense-strand of *Myoparr* (#3 in Figure 3B), but not to the full-length antisense-strand of *Myoparr* (#4). Although deletion of the 5'-region (#5 and 6) or 3'-region (#2 and 7) of *Myoparr* did not affect binding to hnRNPK, the deletion of the 3'-half of *Myoparr* (#1) completely diminished the binding to hnRNPK (Figure 3B). These results indicated that an approximately 300-nt region (613-952 nt) of *Myoparr* is indispensable for binding to hnRNPK. Searching the motif sequence of RBPs from the 300-nt region revealed that there are 8 ccawmcc motifs, which are recognized by hnRNPK (Figure 3C). The deletion of the motifs (660-729 nt) from the full-length of *Myoparr* (#8) markedly weakened the binding to hnRNPK (Figure 3B). Thus, the ccawmcc motifs on *Myoparr* were shown to be required for binding to hnRNPK.

To clarify whether *Myoparr* is involved in regulating the expression of *myogenin* by hnRNPK, we examined the effect of the ccawmcc motif on the *myogenin* promoter activity. To imitate a chromatin structure and epigenetic regulation on the plasmid DNA (Liu et al., 2001), the upstream region of *myogenin* (-1649 to +52) including *Myoparr* was cloned into an episomal luciferase vector. In accordance with our previous findings (Hitachi et al., 2019), the *myogenin* promoter showed high activity in the presence of *Myoparr* (-1650-Luc) in comparison to the -242-Luc construct, which only contains the *myogenin* promoter region in differentiating myoblasts (Figure 3D). Intriguingly, the activity of the -1650-Luc construct was further enhanced by the deletion of a region of approximately 70 bp (1650Δccawmcc-Luc), which corresponds to the 660-729 nt region on *Myoparr* (Figure 3D). These results indicate that hnRNPK represses the expression of *myogenin* through binding to the ccawmcc motif on *Myoparr* during skeletal muscle differentiation.

hnRNPK inhibits skeletal muscle differentiation but is required for normal myotube formation

The inhibitory role of hnRNPK in the expression of *myogenin* via the ccawmcc motif on *Myoparr* suggested that hnRNPK and *Myoparr* have common downstream genes. Our RNA-Seq analysis (Hitachi and Tsuchida, 2019) revealed that *hnRNPK* KD significantly increased the expression of 226 genes and significantly decreased the expression of 190 genes . We compared the downstream genes regulated by *hnRNPK* KD and *Myoparr* KD, and the comparative heatmap analysis showed that the gene regulated by *hnRNPK* KD showed the opposite direction to the *Myoparr* KD (Figure 4A). Twenty percent of genes (84/416) altered by *hnRNPK* KD overlapped with

genes regulated by the *Myoparr* KD (Figure 4B and Supplementary Talbe 2). The intersection of these genes was 12.3-fold greater than that expected by chance ($p = 1.393037 \times 10^{-45}$). Although these 84 genes showed a low correlation coefficient (R=0.0758323), we observed a negative correlation trend for one segment of them, including *myogenin*; the expression of 50 genes belonging to this segment was increased by *hnRNPK* KD and decreased by *Myoparr* KD (red frame in Figure 4C). These genes were enriched in sarcomere organization, myofibril assembly, and muscle contraction categories in GO terms (Figure 4D), indicating that hnRNPK inhibits myogenic differentiation and maturation.

In accordance with the results of the RNA-Seq analysis, we observed a significant increase in the expression of Myosin heavy chain (MHC), which is a later marker of myogenic differentiation and maturation, with *hnRNPK* KD (Figure 4E), indicating the inhibitory role of hnRNPK in myogenic differentiation and maturation. Intriguingly, *hnRNPK* KD did not affect the percentage of differentiated cells; this was shown by the fusion index (Figure 4F) as well as the results from immunocytochemistry to detect myogenin (Figure 2C). Instead, we observed the appearance of locally spherical myotubes following *hnRNPK* KD. These differed from the normal tube-shaped myotubes (Figure 4F). Thus, these results indicated that in addition to its inhibitory role in myogenic differentiation, hnRNPK is required for normal myotube formation.

hnRNPK represses the expression of aminoacyl-tRNA synthetases via the eIF2α/Atf4 pathway

The Venn diagram in Figure 4B indicates that 332 genes regulated by

hnRNPK KD were *Myoparr*-independent, suggesting the *Myoparr*-independent role of hnRNPK in differentiating myoblasts. We performed an enrichment analysis of genes regulated by *hnRNPK* KD and compared them with genes regulated by *Myoparr* KD. As reported previously (Hitachi et al., 2019), genes related to cell cycle and cell division were only enriched in genes regulated by *Myoparr* KD (Figure 5A). Skeletal muscle-associated genes were regulated by both *Myoparr* KD and *hnRNPK* KD (Figure 5A). Intriguingly, genes coding for aminoacyl-tRNA synthetases were regulated specifically by *hnRNPK* KD (red frame in Figure 5A). In mice, there are two-types of aminoacyl-tRNA synthetases: cytosolic and mitochondrial aminoacyl-tRNA synthetase. Our RNA-Seq analysis showed that *hnRNPK* KD significantly increased the expression of 10 genes coding for cytosolic aminoacyl-tRNA synthetases, whereas it had little effect on the expression of genes coding for mitochondrial aminoacyl-tRNA synthetases (Supplementary Figure 2). To confirm the RNA-Seq results, we randomly picked up 5 genes coding for cytosolic aminoacyl-tRNA synthetases, and their expression changes by *hnRNPK* KD were verified by qRT-PCR. *hnRNPK* KD using two distinct siRNAs significantly increased the expression of *Aars*, *Gars*, *Iars*, *Nars*, and *Sars* (Figure 5B-F). This regulation was not observed following *Myoparr* KD (Figure 5B-F), indicating that hnRNPK regulates the expression of these genes in a *Myoparr*-independent manner.

The expression of genes coding for almost all cytosolic aminoacyl-tRNA synthetases is activated by transcription factor Atf4 (Harding et al., 2003; Shan et al., 2016). Thus, we examined whether *hnRNPK* KD altered the expression of Atf4 in skeletal muscle cells. Although not statistically significant, the *Atf4* expression in differentiating myoblasts tended to be increased by *hnRNPK* KD (Figure 5G). *Myoparr* KD did not affect the expression of *Atf4* (Figure 5G). The effect of *hnRNPK* KD was

more pronounced in the expression of Atf4 protein. The amount of Atf4 protein was highly increased by *hnRNPK* KD (Figure 5H). These results suggest that hnRNPK regulates the expression of cytosolic aminoacyl-tRNA synthetases via the expression of Atf4.

Under the condition of endoplasmic reticulum (ER) stress, *Atf4* mRNA is translated more efficiently and contributes to the restoration of cell homeostasis via the regulation of cytosolic aminoacyl-tRNA synthetases (Afroze and Kumar, 2017). Thus, to reveal the molecular mechanism by which hnRNPK regulates the expression of Atf4, we finally focused on ER stress. ISRIB is an inhibitor of eIF2α, which is a downstream component of PERK signaling, one branch of the ER stress sensors. We investigated whether ISRIB treatment could suppress the increase in the expression of Atf4 induced by *hnRNPK* KD and found that ISRIB treatment completely rescued this *hnRNPK*-KD-induced increase (Figure 6A). Furthermore, ISRIB treatment abrogated the increased expression of *Aars*, *Gars*, *Iars*, *Nars*, and *Sars* by *hnRNPK* KD (Figure 6B-F and Supplementary Figure 3A-E). Thus, these results indicate that hnRNPK regulates the expression of cytosolic aminoacyl-tRNA synthetases via the eIF2α/Atf4 pathway during myogenic differentiation.

Discussion

RBPs have multiple molecular functions, including RNA splicing, transcription, translation, RNA stability, and the formation of the nuclear structure, to regulate cell proliferation, differentiation, development, and diseases (Kelaini et al., 2021). Although many RBPs have multiple functions in the cells (Briata and Gherzi, 2020; Jonas et al., 2020; Nostrand et al., 2020), it is still unclear how their pleiotropic

373 functions are determined. In this study, we revealed novel multiple functions of
374 hnRNPK, a member of the hnRNP family of RBPs, in skeletal muscle cells. By
375 focusing on a lncRNA *Myoparr*-associated protein, we found that hnRNPK repressed
376 the expression of *myogenin*, coding for one of the master regulators of muscle
377 differentiation, and inhibited myogenic differentiation through binding to the ccawmcc
378 motif on *Myoparr*. Moreover, our comparative analysis of the downstream genes of
379 hnRNPK and *Myoparr* showed that the function of hnRNPK was heterogenous. During
380 myogenic differentiation, hnRNPK repressed the expression of a set of genes coding for
381 cytosolic aminoacyl-tRNA synthetases via the eIF2α/Atf4 pathway. Taken together, our
382 study revealed multiple inhibitory roles of hnRNPK in skeletal muscle cells: one was
383 lncRNA-dependent and the other was lncRNA-independent (Figure 7). Recently, Xu et
384 al. reported that in hnRNPK, the deficiency of 36 amino acids diminished C2C12
385 differentiation (Xu et al., 2018). However, our results provided strong evidence to
386 support that hnRNPK has an inhibitory effect on muscle differentiation. In addition, we
387 observed the appearance of locally spherical myotubes following *hnRNPK* KD. The
388 morphology of these myotubes closely resembles myotubes with myofibril-assembly
389 defects (Wang et al., 2013), suggesting that hnRNPK may also be involved in the
390 regulation of the myofibril assembly in myotubes. Therefore, despite its
391 lncRNA-dependent and -independent roles in the inhibition of myogenic differentiation,
392 hnRNPK is apparently required for the formation of normal myotubes.

393 We observed that *hnRNPK* KD increased myogenin protein levels more
394 robustly than *myogenin* mRNA. The peak expression of myogenin protein is detected
395 1-2 days after that of *myogenin* mRNA in both *in vitro* and *in vivo* myogenesis (Angelis
396 et al., 1992; Figueroa et al., 2003), suggesting that a slight increase in *myogenin* mRNA

by *hnRNPK* KD in the early stages of myogenic differentiation eventually led to a marked increase in myogenin protein. Therefore, the fine-tuning of the *myogenin* expression by hnRNPK at the early stages of differentiation may have a significant impact on the overall myogenic differentiation processes through the RNA-protein network. Intriguingly, the expression of myogenin protein was increased by *hnRNPK* KD, and the percentage of myogenin-positive cells was not changed, even if *hnRNPK* was depleted. These results suggest that hnRNPK can specifically repress the expression of *myogenin* in a subset of responding cells, rather than by simply turning off the expression of *myogenin* in every myoblast. Our experiments showed that hnRNPK repressed the expression of *myogenin* at the transcriptional level by binding to the ccawmcc motif on *Myoparr*, suggesting that the existence of *Myoparr* would be necessary for hnRNPK to inhibit the expression of *myogenin*. Since *myogenin* and *Myoparr* share the same promoter region (Hitachi et al., 2019), *myogenin* and *Myoparr* are likely expressed in the same cells. Thus, the expression of *myogenin* would not be activated in the cells without the cell-intrinsic expression of *Myoparr*, even if *hnRNPK* is depleted in every myoblast. Further studies are required to investigate the more precise molecular mechanism by which hnRNPK regulates the expression of *myogenin* via binding to *Myoparr*.

ER stress is induced by several perturbations disrupting cell homeostasis, including protein misfolding, viral infection, and changes in intracellular calcium concentration (Hetz et al., 2015). The cells recognize those stresses with three branches of ER transmembrane sensors signaling, PERK, inositol-requiring protein 1 (IRE1), and ATF6 (Afroze and Kumar, 2017). During myogenic differentiation, ATF6 signaling was activated and led to apoptosis in myoblasts (Nakanishi et al., 2005). The increased

421 phosphorylation of eIF2α, a component of PERK signaling, was observed in myoblasts
422 at the early stage after the induction of differentiation (Alter and Bengal, 2011). In
423 addition, treatment with ER stress inducers enhanced apoptosis in myoblasts but led to
424 efficient myogenic differentiation in the remaining surviving cells (Nakanishi et al.,
425 2007). Recently, the deletion of PERK in satellite cells, which are adult muscle stem
426 cells, was shown to inhibit myogenic differentiation and led to impaired skeletal muscle
427 regeneration in adult mice (Xiong et al., 2017), indicating that ER stress promotes
428 myogenic differentiation. In this study, we showed that the *hnRNPK* KD in
429 differentiating myoblasts increased the expression of Atf4 and this effect was
430 diminished by treatment with ISRIB, a specific inhibitor of eIF2α. The expression levels
431 of a set of genes coding for cytosolic aminoacyl-tRNA synthetases, which are regulated
432 by Atf4, were also increased by the *hnRNPK* KD, and were completely rescued after
433 ISRIB treatment. The inhibitory effects of hnRNPK on Atf4 and cytosolic
434 aminoacyl-tRNA synthetases were independent of *Myoparr*. Therefore, our findings
435 suggest that hnRNPK fine-tunes the myogenic differentiation process by modulating ER
436 stress via eIF2α/Atf4 signaling in a lncRNA-independent manner. Since hnRNPK is
437 involved in the translational efficiency (Lynch et al., 2005; Yano et al., 2005), a
438 decrease in hnRNPK may induce the unfolded protein response via the translational
439 machinery in myoblasts and alter eIF2α/Atf4 signaling.

440 In conclusion, hnRNPK plays multiple lncRNA-dependent and -independent
441 roles in the inhibition of myogenic differentiation. Thus, the analysis of RBPs bound to
442 lncRNAs will be useful for elucidating both the physiological functions of lncRNAs and
443 the complex functions of RBPs in cell differentiation. Intriguingly, the *myogenin* gene is
444 responsible for the skeletal muscle atrophy caused by denervation (Moresi et al., 2010).

Atf4 is also involved in skeletal muscle atrophy caused by aging, fasting, and immobilization (Ebert et al., 2012; Ebert et al., 2015). Induced ER stress, including increased PERK signaling, was observed in skeletal muscle biopsy samples from myotonic dystrophy 1 patients and in mdx mice, a model of Duchenne muscular dystrophy (Hulmi et al., 2016; Ikezoe et al., 2007). Moreover, mutations in genes coding for aminoacyl-tRNA synthetases are implicated in human neuromuscular disorders (Benarroch et al., 2020), and autoantibodies against aminoacyl-tRNA synthetases are found in autoimmune disease (Targoff et al., 1993). Collectively, downstream genes of hnRNPK are strongly associated with neuromuscular and other disorders in humans, suggesting that targeting hnRNPK to regulate the expression of these genes and signaling may become a new therapeutic strategy for human diseases.

Acknowledgments

This work was supported in part by JSPS KAKENHI (19H03427 and 20K07315), Intramural Research Grants (2-5) for Neurological and Psychiatric Disorders of NCNP, and a Grant-in-Aid from the Mochida Memorial Foundation for Medical and Pharmaceutical Research.

Author Contributions

K.H. and K.T. designed research; K.H. analyzed data; K.H., Y.K., and M.N. performed research; K.H. and K.T. wrote the paper. All authors revised, edited, and read the manuscript and approved the final manuscript.

Conflict of interest

The authors declare no competing interests in association with the present study.

Figure Legends

Figure 1. Intracellular interaction between *Myoparr* and hnRNPK in differentiating C2C12 cells. (A) Synthesized *Myoparr* was mixed with C2C12 nuclear extract. Following purification of *Myoparr* by immunoprecipitation, the interaction between *Myoparr* and hnRNPK was confirmed by immunoblotting using an hnRNPK-specific antibody. *EGFP* mRNA was used for the control. Note that the smaller band would be a splicing isoform of hnRNPK (Makeyev and Liebhaber, 2002). (B) RNA immunoprecipitation for *Myoparr* and *Xist* in differentiating C2C12 cells by an hnRNPK antibody. The interaction between endogenous *Myoparr* and hnRNPK was detected by qRT-PCR. Normal rabbit IgG was used for the control. The presence or absence of reverse transcription reaction is shown by (RT+) or (RT-), respectively. n = 4, mean ± SD. ***$p < 0.001$. (C) hnRNPK protein from C2C12 cells purified by immunoprecipitation in (B) was confirmed by Western blotting.

Figure 2. hnRNPK represses the expression of myogenin at the transcriptional level. (A-B) Western blots showing the hnRNPK and myogenin expression during C2C12 differentiation (A) and in C2C12 cells 48 h after *hnRNPK* KD (B). The tubulin expression served as an internal control. n = 3. (C) Immunocytochemistry for myogenin 48 h after *hnRNPK* KD in C2C12 cells. Nuclei were counterstained with DAPI. Bar, 100 μm. The percentage of the myogenin-positive cells is shown as the percentage of the control. n = 4, mean ± SD. n.s., not significant. (D-E) Quantitative RT-PCR to detect the expression of *hnRNPK* (D), *myogenin* (E), and *Myoparr* (F) after *hnRNPK*

knockdown. n = 3-4, mean ± SD. ***$p < 0.001$, *$p < 0.05$, n.s., not significant. (G) Exogenous hnRNPK decreased the promoter activity of *myogenin* in differentiating C2C12 cells. n = 3, mean ± SD. *$p < 0.05$.

Figure 3. hnRNPK represses the expression of *myogenin* via binding to *Myoparr*. (A) A schematic diagram of various lengths of *Myoparr* used for RNA pull-down assays. (B) *In vitro* transcribed/translated hnRNPK protein was pulled down by *Myoparr* and then detected by Western blotting using an hnRNPK-specific antibody. Lane numbers are consistent with (A). The RNA lanes indicate various forms of *Myoparr* used for RNA pull-down. (C) The results of an RBPmap analysis searching the motif of hnRNPK. Colored letters correspond to the hnRNPK motif. The red frame indicates the ccawmcc motifs within the region deleted in Δccawmcc, #8 in (A). (D) The left panel shows a schematic diagram of the constructs used for the luciferase assays. -242-Luc contains the *myogenin* promoter region. -1650-Luc contains both the *myogenin* promoter region and *Myoparr*. -1650Δccawmcc-Luc contains the *myogenin* promoter region and *Myoparr* without the ccawmcc motifs, corresponding to #8 in A. The right panel shows the relative luciferase activities of indicated constructs in differentiating C2C12 cells. n = 4, mean ± SD. ***$p < 0.001$, **$p < 0.01$, *$p < 0.05$.

Figure 4. hnRNPK inhibits myogenic differentiation but is required for normal myotube formation. (A) A heatmap diagram showing the increased or decreased expression of genes regulated by *Myoparr* KD and *hnRNPK* KD. (B) The intersection of genes regulated by *Myoparr* KD and *hnRNPK* KD shows a significant (Fisher's exact test) overlap, which is 12.3 times larger than would be expected by chance alone. (C)

Eighty-four genes with expression levels that were significantly altered by both *Myoparr* KD and *hnRNPK* KD showed an un-correlated pattern (R = 0.0758323, log 2 ratio scale). The red frame indicates the 50 genes for which the expression was decreased by *Myoparr* KD but increased by *hnRNPK* KD. (D) Enrichment GO categories of the 50 genes, corresponding to the red frame in (C). (E) Western blot showing the increased expression of MHC in C2C12 myotubes after *hnRNPK* KD. The tubulin expression served as an internal control. n = 3. (F) Immunocytochemistry for MHC 72 h after *hnRNPK* KD. Nuclei were counterstained with DAPI. Bar, 100 μm. The fusion index is shown as the percent of the control. n = 3, mean ± SD. n.s., not significant.

Figure 5. hnRNPK regulates the expression of genes coding for aminoacyl-tRNA synthetases in a *Myoparr*-independent manner. (A) A Metascape analysis of genes regulated by *Myoparr* KD and *hnRNPK* KD. The red frame indicates the GO terms that were specifically enriched in *hnRNPK* KD. (B-G) qRT-PCR to detect the expression of *Aars* (B), *Gars* (C), *Iars* (D), *Nars* (E), *Sars* (F), *Atf4* (G) after either *Myoparr* KD or *hnRNPK* KD. n = 3, mean ± SD. $^{**}p < 0.01$, $^{*}p < 0.05$, n.s., not significant. (H) Western blot showing the increased expression of Atf4 by *hnRNPK* KD. The tubulin expression served as an internal control. n = 3.

Figure 6. hnRNPK regulates the expression of genes coding for aminoacyl-tRNA synthetases via the eIF2α/Atf4 pathway. (A) Western blot showing the increased Atf4 expression after *hnRNPK* KD, and ISRIB treatment suppressed the increase. DMSO is used as a control. n = 3. (B-F) qRT-PCR to detect the expression of *Aars* (B), *Gars* (C),

Iars (D), *Nars* (E), *Sars* (F) after *hnRNPK* KD and ISRIB treatment. n = 3, mean ± SD. $^{**}p < 0.01$, $^{*}p < 0.05$, n.s., not significant.

Figure 7. Multiple inhibitory roles of hnRNPK during myogenic differentiation. During myogenic differentiation, hnRNPK has two different downstream targets. One is *myogenin*, which codes for a regulator of myogenic differentiation. hnRNPK represses the *myogenin* expression by binding to the ccawmcc motifs on *Myoparr*. The other target is aminoacyl-tRNA synthetases. hnRNPK regulates the expression of aminoacyl-tRNA synthetases via the eIF2α/Atf4 pathway. In hnRNPK-depleted cells, the hyperactivated expression of these genes may lead to the locally spherical formation of myotubes.

Supplementary Table 1. Primer and siRNA sequences.

Supplementary Table 2. The value (log2 fold change) of the genes for which expression levels were increased or decreased by *Myoparr* KD and *hnRNPK* KD.

Supplementary Figure 1. Detection of the interaction between *Myoparr* and TIAR in differentiating C2C12 cells. (A) The interaction between synthesized *Myoparr* and TIAR was detected by immunoblotting using a TIAR antibody. (B) qRT-PCR for the detection of *Myoparr* and *Xist* following RNA-immunoprecipitation using a TIAR antibody. The presence or absence of reverse transcription reaction is shown by (RT+) or (RT-), respectively. Bars indicate the average of two independent experiments, and circles and triangles represent the values of each experiment. (C) Purified TIAR protein

from C2C12 cells by immunoprecipitation using a TIAR antibody was confirmed by Western blotting.

Supplementary Figure 2. RNA-Seq revealed the altered expression of a group of genes coding for cytosolic aminoacyl-tRNA synthetases by *hnRNPK* KD. (A) The KEGG pathway diagram of cytosolic aminoacyl-tRNA biosynthesis. The gene names surrounded by the red frame indicate genes that are significantly upregulated by *hnRNPK* KD. (B-C) The results of the RNA-Seq analysis showing the altered expression of genes coding for cytosolic aminoacyl-tRNA synthetases (B) and mitochondrial aminoacyl-tRNA synthetases (C) by *hnRNPK* KD. Red and blue indicate genes that are significantly upregulated or downregulated, respectively, by *hnRNPK* KD.

Supplementary Figure 3. hnRNPK regulates the expression of a group of genes coding for aminoacyl-tRNA synthetases via the eIF2α/Atf4 pathway. (A-E) The results of qRT-PCR for detecting the altered expression of *Aars* (A), *Gars* (B), *Iars* (C), *Nars* (D), *Sars* (E) following *hnRNPK* KD (using a different siRNA from Figure 6) and ISRIB treatment. n = 3, mean ± SD. *$p < 0.05$.

References

Afroze, D. and Kumar, A. (2017). ER stress in skeletal muscle remodeling and myopathies. *Febs J* **286**, 379–398.

Alter, J. and Bengal, E. (2011). Stress-induced C/EBP Homology Protein (CHOP) represses MyoD transcription to delay myoblast differentiation. *Plos One* **6**, e29498.

Angelis, M. G. C.-D., Lyons, G., Sonnino, C., Angelis, L. D., Vivarelli, E., Farmer,

K., Wright, W. E., Molinaro, M., Bouchè, M. and Buckingham, M. (1992). MyoD, myogenin independent differentiation of primordial myoblasts in mouse somites. *J Cell Biology* **116**, 1243−1255.

Benarroch, L., Bonne, G., Rivier, F. and Hamroun, D. (2020). The 2021 version of the gene table of neuromuscular disorders (nuclear genome). *Neuromuscular Disord* **30**, 1008−1048.

Bomsztyk, K., Denisenko, O. and Ostrowski, J. (2004). hnRNP K: One protein multiple processes. *Bioessays* **26**, 629−638.

Briata, P. and Gherzi, R. (2020). Long non-coding RNA-ribonucleoprotein networks in the post-transcriptional control of gene expression. *Non-coding Rna* **6**, 40.

Caretti, G., Schiltz, R. L., Dilworth, F. J., Padova, M. D., Zhao, P., Ogryzko, V., Fuller-Pace, F. V., Hoffman, E. P., Tapscott, S. J. and Sartorelli, V. (2006). The RNA helicases p68/p72 and the noncoding RNA SRA are coregulators of MyoD and skeletal muscle differentiation. *Dev Cell* **11**, 547−560.

Chakraborty, S., Deb, A., Maji, R. K., Saha, S. and Ghosh, Z. (2014). LncRBase: An enriched resource for lncRNA information. *Plos One* **9**, e108010.

Chu, C., Zhang, Q. C., da Rocha, S. T., Flynn, R. A., Bharadwaj, M., Calabrese, J. M., Magnuson, T., Heard, E. and Chang, H. Y. (2015). Systematic discovery of Xist RNA binding proteins. *Cell* **161**, 404−416.

Dimitrova, N., Zamudio, J. R., Jong, R. M., Soukup, D., Resnick, R., Sarma, K., Ward, A. J., Raj, A., Lee, J. T., Sharp, P. A., et al. (2014). LincRNA-p21 activates p21 in cis to promote polycomb target gene expression and to enforce the G1/S checkpoint. *Mol Cell* **54**, 777−790.

Ebert, S. M., Dyle, M. C., Kunkel, S. D., Bullard, S. A., Bongers, K. S., Fox, D. K., Dierdorff, J. M., Foster, E. D. and Adams, C. M. (2012). Stress-induced skeletal muscle Gadd45a expression reprograms myonuclei and causes muscle atrophy. *J Biol Chem* **287**, 27290−27301.

Ebert, S. M., Dyle, M. C., Bullard, S. A., Dierdorff, J. M., Murry, D. J., Fox, D. K., Bongers, K. S., Lira, V. A., Meyerholz, D. K., Talley, J. J., et al. (2015). Identification and small molecule inhibition of an activating transcription factor 4 (ATF4)-dependent pathway to age-related skeletal muscle weakness and atrophy. *J Biol Chem* **290**, 25497−25511.

Figueroa, A., Cuadrado, A., Fan, J., Atasoy, U., Muscat, G. E., Muñoz-Canoves, P.,

Gorospe, M. and Muñoz, A. (2003). Role of HuR in skeletal myogenesis through coordinate regulation of muscle differentiation genes. *Mol Cell Biol* **23**, 4991–5004.

Gebauer, F., Schwarzl, T., Valcárcel, J. and Hentze, M. W. (2021). RNA-binding proteins in human genetic disease. *Nat Rev Genet* **22**, 185–198.

Gerstberger, S., Hafner, M. and Tuschl, T. (2014). A census of human RNA-binding proteins. *Nat Rev Genet* **15**, 829–845.

Harding, H. P., Zhang, Y., Zeng, H., Novoa, I., Lu, P. D., Calfon, M., Sadri, N., Yun, C., Popko, B., Paules, R., et al. (2003). An integrated stress response regulates amino acid metabolism and resistance to oxidative stress. *Mol Cell* **11**, 619–633.

Hetz, C., Chevet, E. and Oakes, S. A. (2015). Proteostasis control by the unfolded protein response. *Nat Cell Biol* **17**, 829–838.

Hirose, T., Yamazaki, T. and Nakagawa, S. (2019). Molecular anatomy of the architectural NEAT1 noncoding RNA: The domains, interactors, and biogenesis pathway required to build phase‐separated nuclear paraspeckles. *Wiley Interdiscip Rev Rna* **10**, e1545.

Hitachi, K. and Tsuchida, K. (2019). Data describing the effects of depletion of Myoparr, myogenin, Ddx17, and hnRNPK in differentiating C2C12 cells. *Data Brief* **25**, 104172.

Hitachi, K. and Tsuchida, K. (2020). The Chemical Biology of Long Noncoding RNAs. *Rna Technologies* 431–463.

Hitachi, K., Nakatani, M., Takasaki, A., Ouchi, Y., Uezumi, A., Ageta, H., Inagaki, H., Kurahashi, H. and Tsuchida, K. (2019). Myogenin promoter-associated lncRNA Myoparr is essential for myogenic differentiation. *Embo Rep* **20**, e47468.

Hon, C.-C., Ramilowski, J. A., Harshbarger, J., Bertin, N., Rackham, O. J. L., Gough, J., Denisenko, E., Schmeier, S., Poulsen, T. M., Severin, J., et al. (2017). An atlas of human long non-coding RNAs with accurate 5′ ends. *Nature* **543**, 199–204.

Howarth, M. M., Simpson, D., Ngok, S. P., Nieves, B., Chen, R., Siprashvili, Z., Vaka, D., Breese, M. R., Crompton, B. D., Alexe, G., et al. (2014). Long noncoding RNA EWSAT1-mediated gene repression facilitates Ewing sarcoma oncogenesis. *J Clin Invest* **124**, 5275–5290.

Hulmi, J. J., Hentilä, J., DeRuisseau, K. C., Oliveira, B. M., Papaioannou, K. G., Autio, R., Kujala, U. M., Ritvos, O., Kainulainen, H., Korkmaz, A., et al. (2016).

Effects of muscular dystrophy, exercise and blocking activin receptor IIB ligands on the unfolded protein response and oxidative stress. *Free Radical Bio Med* **99**, 308–322.

Ikezoe, K., Nakamori, M., Furuya, H., Arahata, H., Kanemoto, S., Kimura, T., Imaizumi, K., Takahashi, M. P., Sakoda, S., Fujii, N., et al. (2007). Endoplasmic reticulum stress in myotonic dystrophy type 1 muscle. *Acta Neuropathol* **114**, 527–535.

Jonas, K., Calin, G. A. and Pichler, M. (2020). RNA-binding proteins as important regulators of long non-coding RNAs in cancer. *Int J Mol Sci* **21**, 2969.

Kanehisa, M., Furumichi, M., Sato, Y., Ishiguro-Watanabe, M. and Tanabe, M. (2020). KEGG: integrating viruses and cellular organisms. *Nucleic Acids Res* **49**, D545-D551.

Kataruka, S., Akhade, V. S., Kayyar, B. and Rao, M. R. S. (2017). Mrhl long noncoding RNA mediates meiotic commitment of mouse spermatogonial cells by regulating Sox8 expression. *Mol Cell Biol* **37**, e00632-16.

Kelaini, S., Chan, C., Cornelius, V. A. and Margariti, A. (2021). RNA-binding proteins hold key roles in function, dysfunction, and disease. *Biology* **10**, 366.

Legnini, I., Morlando, M., Mangiavacchi, A., Fatica, A. and Bozzoni, I. (2014). A feedforward regulatory loop between HuR and the long noncoding RNA linc-MD1 controls early phases of myogenesis. *Mol Cell* **53**, 506–514.

Liu, R., Liu, H., Chen, X., Kirby, M., Brown, P. O. and Zhao, K. (2001). Regulation of CSF1 promoter by the SWI/SNF-like BAF complex. *Cell* **106**, 309–318.

Love, M. I., Huber, W. and Anders, S. (2014). Moderated estimation of fold change and dispersion for RNA-seq data with DESeq2. *Genome Biol* **15**, 550.

Lynch, M., Chen, L., Ravitz, M. J., Mehtani, S., Korenblat, K., Pazin, M. J. and Schmidt, E. V. (2005). hnRNP K binds a core polypyrimidine element in the eukaryotic translation initiation Factor 4E (eIF4E) promoter, and its regulation of eIF4E contributes to neoplastic transformation. *Mol Cell Biol* **25**, 6436–6453.

Ma, L., Cao, J., Liu, L., Du, Q., Li, Z., Zou, D., Bajic, V. B. and Zhang, Z. (2019). LncBook: a curated knowledgebase of human long non-coding RNAs. *Nucleic Acids Res* **47**, D128-D134.

Makeyev, A. V. and Liebhaber, S. A. (2002). The poly(C)-binding proteins: A

multiplicity of functions and a search for mechanisms. *Rna* **8**, 265−278.

Moresi, V., Williams, A. H., Meadows, E., Flynn, J. M., Potthoff, M. J., McAnally, J., Shelton, J. M., Backs, J., Klein, W. H., Richardson, J. A., et al. (2010). Myogenin and class II HDACs control neurogenic muscle atrophy by inducing E3 ubiquitin ligases. *Cell* **143**, 35−45.

Nakanishi, K., Sudo, T. and Morishima, N. (2005). Endoplasmic reticulum stress signaling transmitted by ATF6 mediates apoptosis during muscle development. *J Cell Biology* **169**, 555−560.

Nakanishi, K., Dohmae, N. and Morishima, N. (2007). Endoplasmic reticulum stress increases myofiber formation in vitro. *Faseb J* **21**, 2994−3003.

Nostrand, E. L. V., Freese, P., Pratt, G. A., Wang, X., Wei, X., Xiao, R., Blue, S. M., Chen, J.-Y., Cody, N. A. L., Dominguez, D., et al. (2020). A large-scale binding and functional map of human RNA-binding proteins. *Nature* **583**, 711−719.

Paz, I., Kosti, I., Ares, M., Cline, M. and Mandel-Gutfreund, Y. (2014). RBPmap: a web server for mapping binding sites of RNA-binding proteins. *Nucleic Acids Res* **42**, W361−W367.

Sallam, T., Jones, M., Thomas, B. J., Wu, X., Gilliland, T., Qian, K., Eskin, A., Casero, D., Zhang, Z., Sandhu, J., et al. (2018). Transcriptional regulation of macrophage cholesterol efflux and atherogenesis by a long noncoding RNA. *Nat Med* **24**, 304−312.

Shan, J., Zhang, F., Sharkey, J., Tang, T. A., Örd, T. and Kilberg, M. S. (2016). The C/ebp-Atf response element (CARE) location reveals two distinct Atf4-dependent, elongation-mediated mechanisms for transcriptional induction of aminoacyl-tRNA synthetase genes in response to amino acid limitation. *Nucleic Acids Res* **44**, 9719−9732.

Statello, L., Guo, C.-J., Chen, L.-L. and Huarte, M. (2021). Gene regulation by long non-coding RNAs and its biological functions. *Nat Rev Mol Cell Bio* **22**, 96−118.

Tang, S., Xie, Z., Wang, P., Li, J., Wang, S., Liu, W., Li, M., Wu, X., Su, H., Cen, S., et al. (2018). LncRNA-OG promotes the osteogenic differentiation of bone marrow-derived mesenchymal stem cells under the regulation of hnRNPK. *Stem Cells* **37**, 270−283.

Targoff, I. N., Trieu, E. P. and Miller, F. W. (1993). Reaction of anti-OJ autoantibodies with components of the multi-enzyme complex of aminoacyl-tRNA

synthetases in addition to isoleucyl-tRNA synthetase. *J Clin Invest* **91**, 2556−2564.

Wang, Z., Cui, J., Wong, W. M., Li, X., Xue, W., Lin, R., Wang, J., Wang, P., Tanner, J. A., Cheah, K. S. E., et al. (2013). Kif5b controls the localization of myofibril components for their assembly and linkage to the myotendinous junctions. *Development* **140**, 617−626.

Wang, Z., Qiu, H., He, J., Liu, L., Xue, W., Fox, A., Tickner, J. and Xu, J. (2020). The emerging roles of hnRNPK. *J Cell Physiol* **235**, 1995−2008.

Xiong, G., Hindi, S. M., Mann, A. K., Gallot, Y. S., Bohnert, K. R., Cavener, D. R., Whittemore, S. R. and Kumar, A. (2017). The PERK arm of the unfolded protein response regulates satellite cell-mediated skeletal muscle regeneration. *Elife* **6**, e22871.

Xu, Y., Li, R., Zhang, K., Wu, W., Wang, S., Zhang, P. and Xu, H. (2018). The multifunctional RNA-binding protein hnRNPK is critical for the proliferation and differentiation of myoblasts. 350−355.

Yano, M., Okano, H. J. and Okano, H. (2005). Involvement of Hu and heterogeneous nuclear ribonucleoprotein K in neuronal differentiation through p21 mRNA post-transcriptional regulation. *J Biol Chem* **280**, 12690−12699.

Yoon, J.-H., Abdelmohsen, K., Srikantan, S., Yang, X., Martindale, J. L., De, S., Huarte, M., Zhan, M., Becker, K. G. and Gorospe, M. (2012). LincRNA-p21 suppresses target mRNA translation. *Mol Cell* **47**, 648−655.

Zhou, Y., Zhou, B., Pache, L., Chang, M., Khodabakhshi, A. H., Tanaseichuk, O., Benner, C. and Chanda, S. K. (2019). Metascape provides a biologist-oriented resource for the analysis of systems-level datasets. *Nat Commun* **10**, 1523.

Figure 1

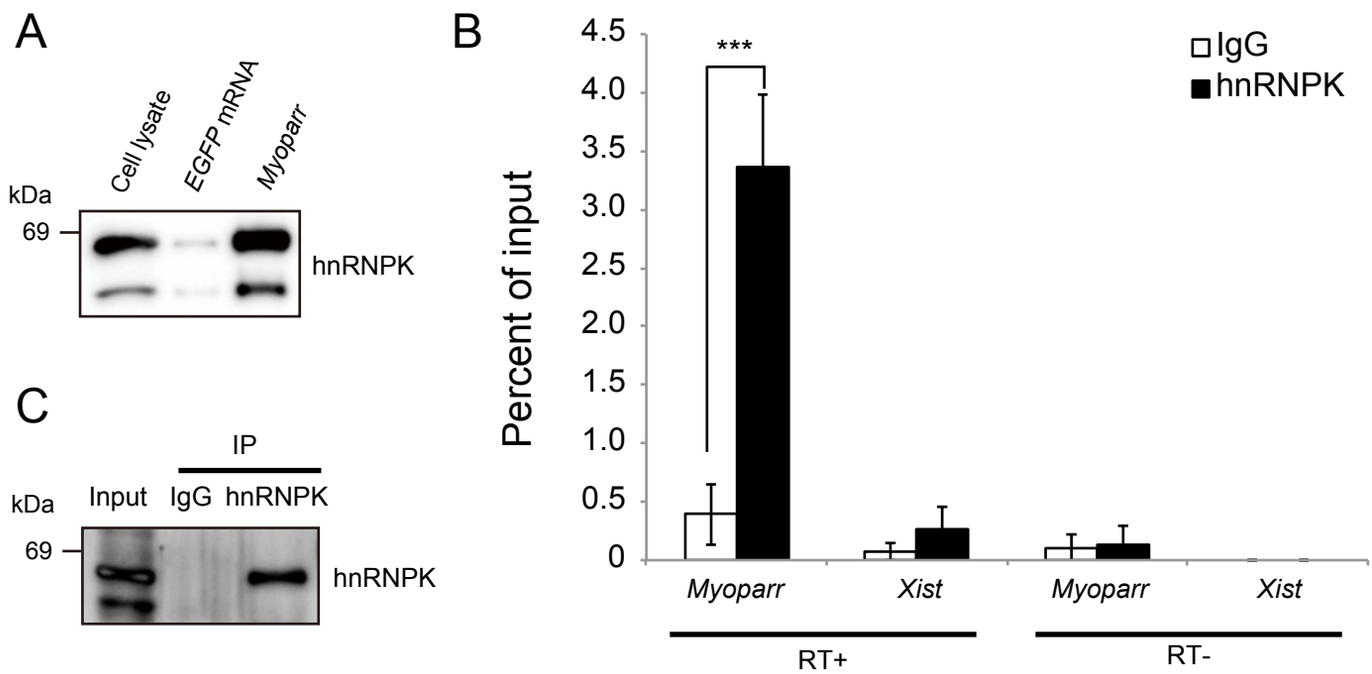
A
Cell lysate
EGFP mRNA
Myoparr
kDa
69
hnRNPK
B
Percent of input
4.5
4.0
3.5
3.0
2.5
2.0
1.5
1.0
0.5
0
***
IgG
hnRNPK
Myoparr
Xist
Myoparr
Xist
RT+
RT-
C
IP
kDa
Input
IgG
hnRNPK
69
hnRNPK

Figure 2

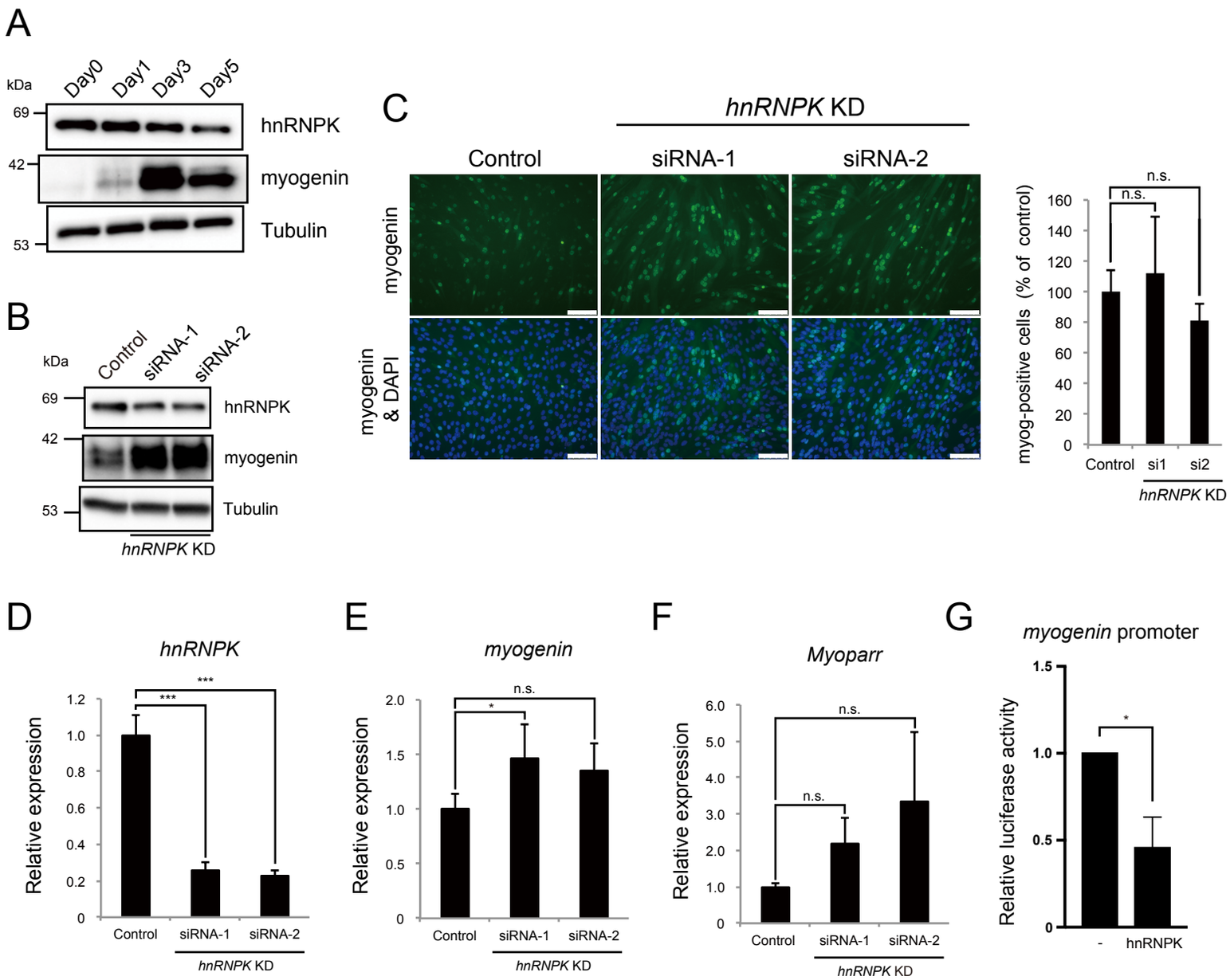
A
kDa
Day0
Day1
Day3
Day5
69
42
53
hnRNPK
myogenin
Tubulin
B
kDa
Control
siRNA-1
siRNA-2
69
42
53
hnRNPK
myogenin
Tubulin
hnRNPK KD
C
hnRNPK KD
Control
siRNA-1
siRNA-2
myogenin
myogenin & DAPI
myog-positive cells (% of control)
n.s.
n.s.
Control
si1
si2
hnRNPK KD
D
hnRNPK
Relative expression
***
***
Control
siRNA-1
siRNA-2
hnRNPK KD
E
myogenin
Relative expression
n.s.
*
Control
siRNA-1
siRNA-2
hnRNPK KD
F
Myoparr
Relative expression
n.s.
n.s.
Control
siRNA-1
siRNA-2
hnRNPK KD
G
myogenin promoter
Relative luciferase activity
*
-
hnRNPK

Figure 3

A

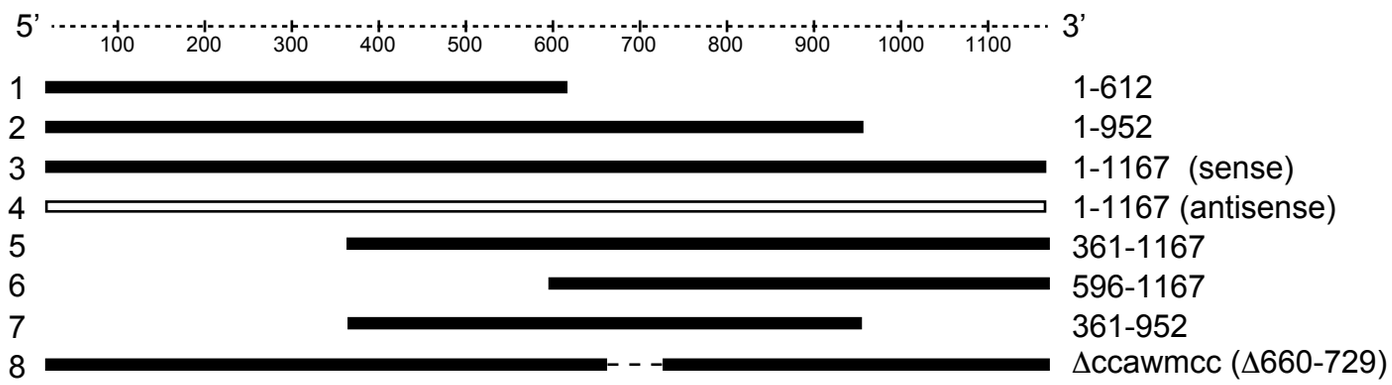

B

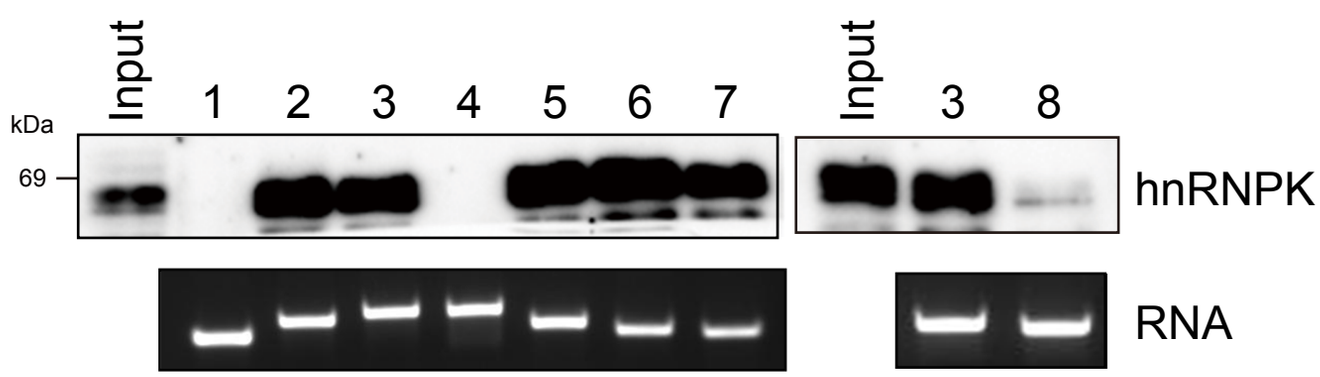

C

Protein: HNRNPK(Hs/Mm)

Position	Motif	Occurrence	Z-score	P-value
274	ccawmcc	gucaguccc**aug**agacccc**uaaaga**ccuacc**a**cuaccacaucaggaccacuccagau	2.420	7.76e-03
295	ccawmcc	aagaccuaccacuaccacaucagga**ccacucc**agauuuggggcgugugu

Figure 4

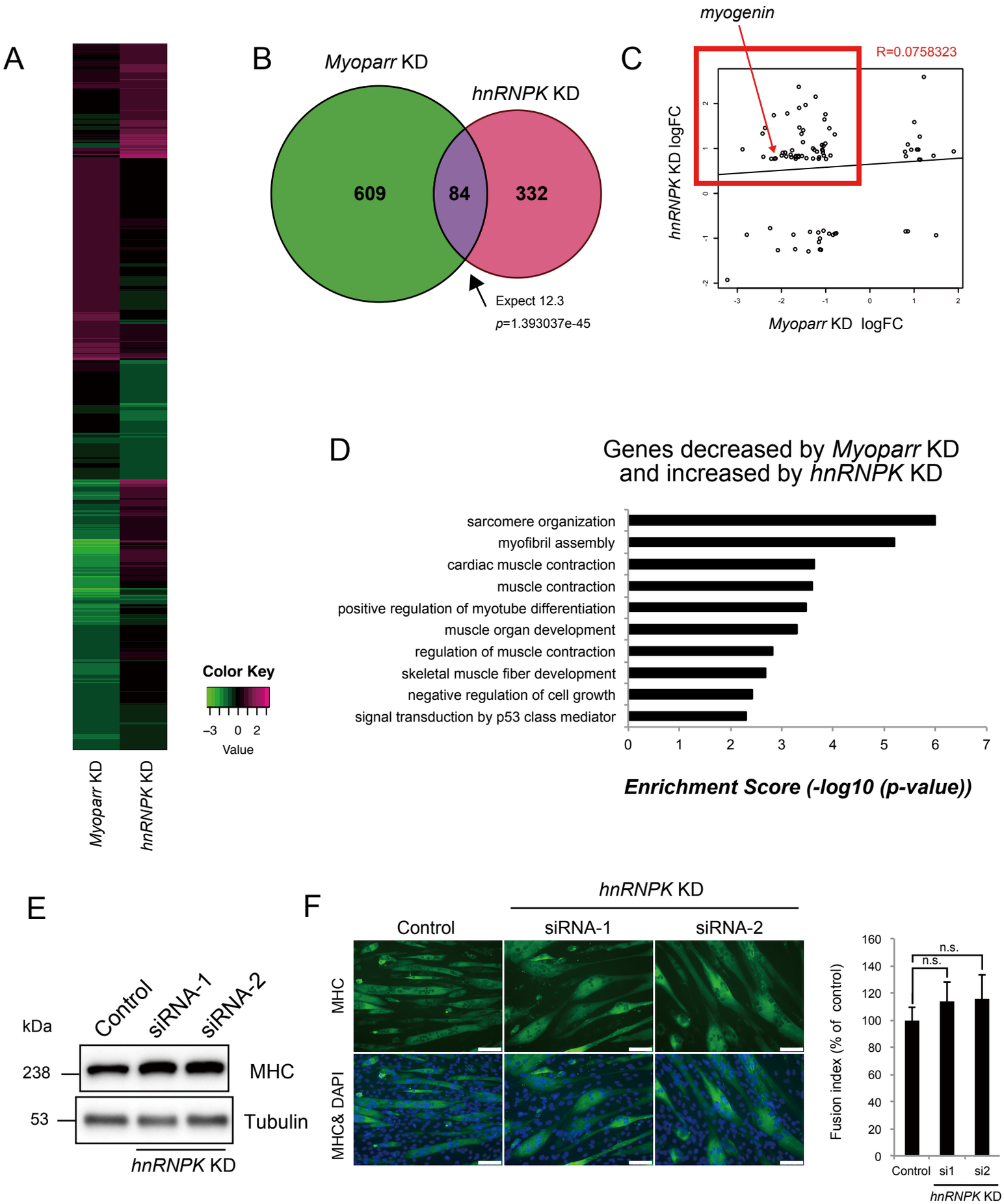
A
Myoparr KD
hnRNPK KD
Color Key
−3 0 2
Value
B
Myoparr KD
hnRNPK KD
609
84
332
Expect 12.3
p=1.393037e-45
C
myogenin
R=0.0758323
hnRNPK KD logFC
Myoparr KD logFC
D
Genes decreased by Myoparr KD and increased by hnRNPK KD
sarcomere organization
myofibril assembly
cardiac muscle contraction
muscle contraction
positive regulation of myotube differentiation
muscle organ development
regulation of muscle contraction
skeletal muscle fiber development
negative regulation of cell growth
signal transduction by p53 class mediator
0 1 2 3 4 5 6 7
Enrichment Score (-log10 (p-value))
E
kDa
Control
siRNA-1
siRNA-2
238
MHC
53
Tubulin
hnRNPK KD
F
hnRNPK KD
Control
siRNA-1
siRNA-2
MHC
MHC& DAPI
Fusion index (% of control)
160
140
120
100
80
60
40
20
0
n.s.
n.s.
Control
si1
si2
hnRNPK KD

Figure 5

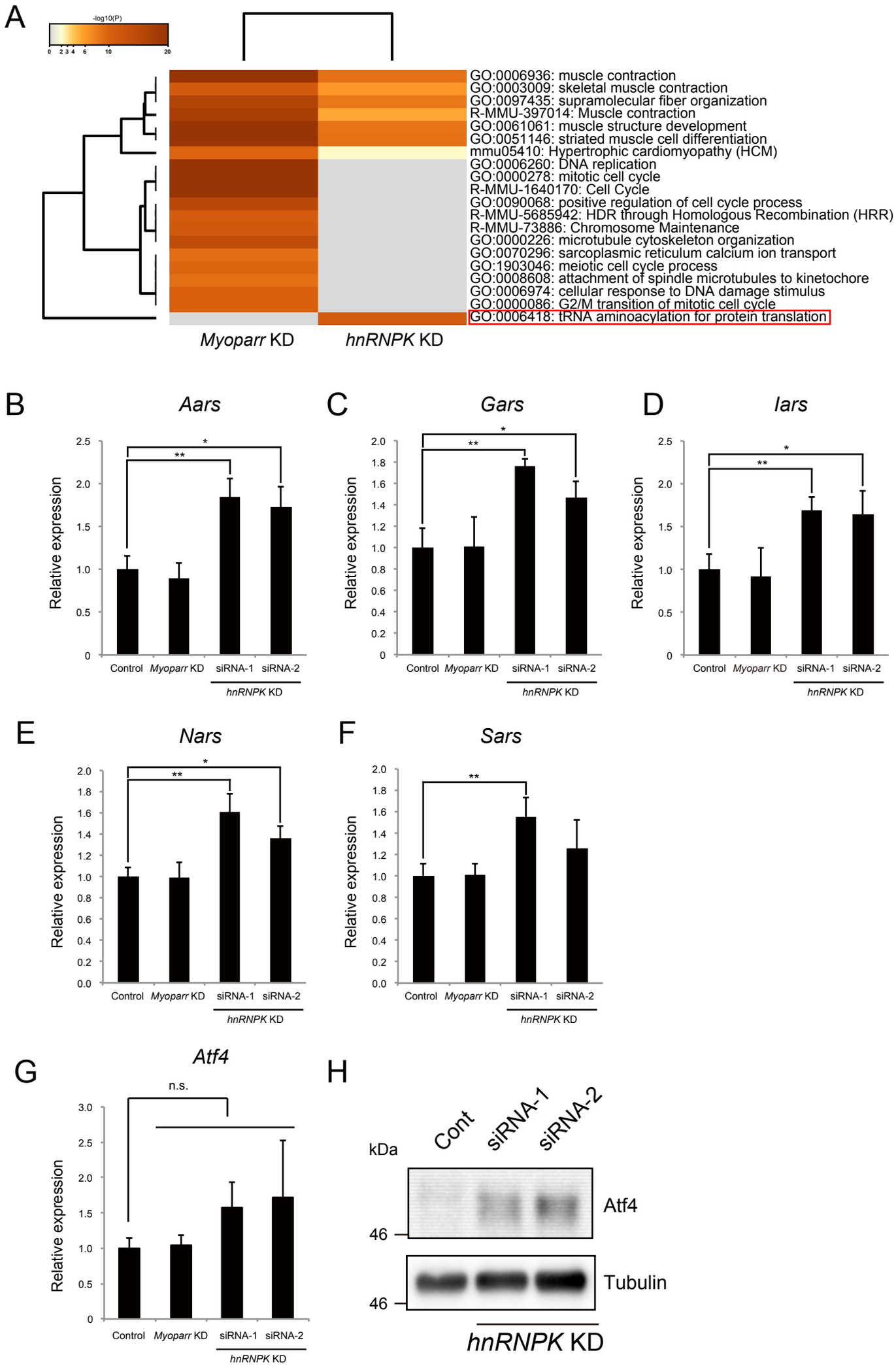
A
-log10(P)
0 2 3 4 6 10 20
GO:0006936: muscle contraction
GO:0003009: skeletal muscle contraction
GO:0097435: supramolecular fiber organization
R-MMU-397014: Muscle contraction
GO:0061061: muscle structure development
GO:0051146: striated muscle cell differentiation
mmu05410: Hypertrophic cardiomyopathy (HCM)
GO:0006260: DNA replication
GO:0000278: mitotic cell cycle
R-MMU-1640170: Cell Cycle
GO:0090068: positive regulation of cell cycle process
R-MMU-5685942: HDR through Homologous Recombination (HRR)
R-MMU-73886: Chromosome Maintenance
GO:0000226: microtubule cytoskeleton organization
GO:0070296: sarcoplasmic reticulum calcium ion transport
GO:1903046: meiotic cell cycle process
GO:0008608: attachment of spindle microtubules to kinetochore
GO:0006974: cellular response to DNA damage stimulus
GO:0000086: G2/M transition of mitotic cell cycle
GO:0006418: tRNA aminoacylation for protein translation
Myoparr KD
hnRNPK KD
B
Aars
C
Gars
D
Iars
E
Nars
F
Sars
Relative expression
Control
Myoparr KD
siRNA-1
siRNA-2
hnRNPK KD
G
Atf4
n.s.
H
kDa
Cont
siRNA-1
siRNA-2
Atf4
Tubulin
46
46
hnRNPK KD

Figure 6

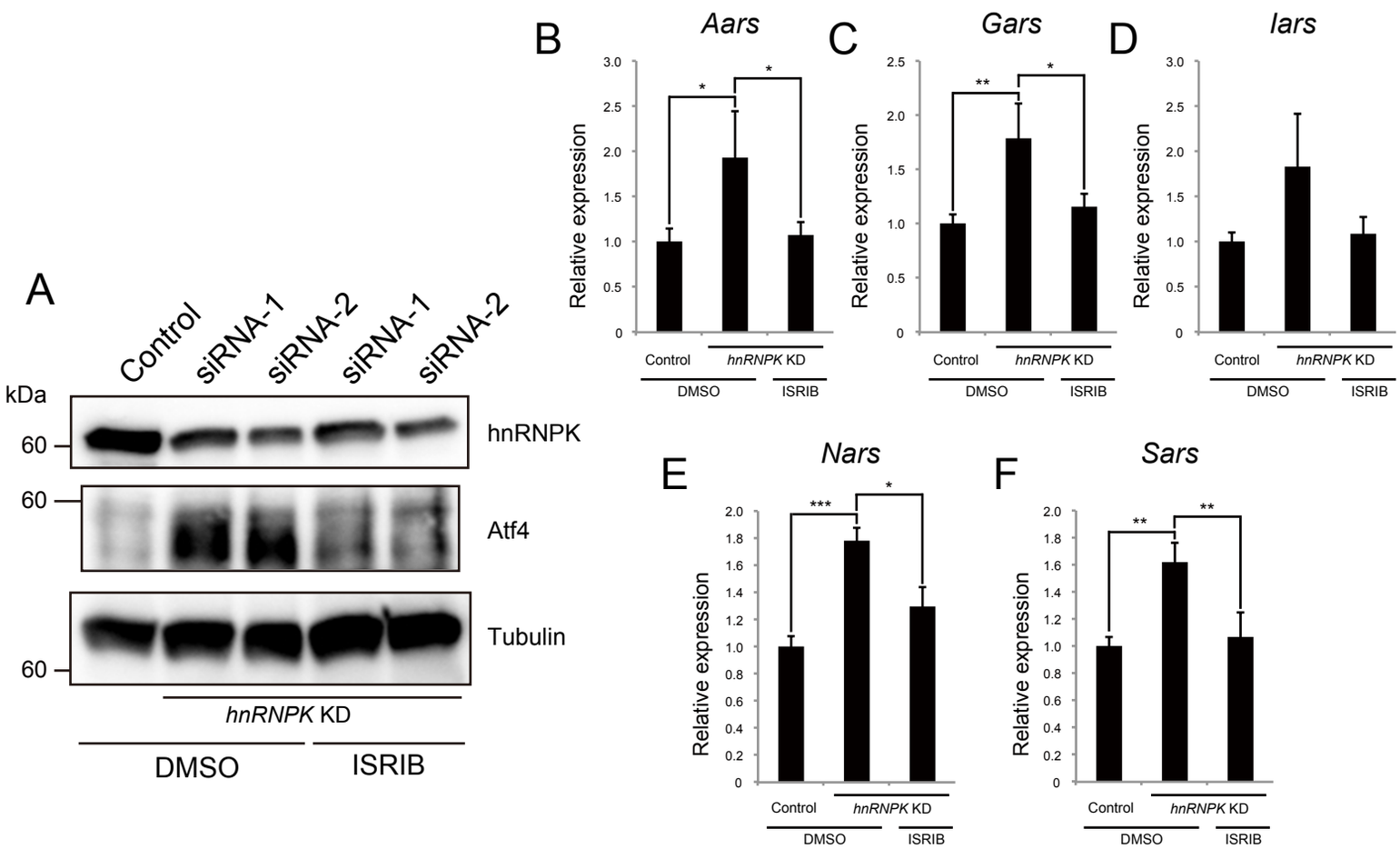
A
Control
siRNA-1
siRNA-2
siRNA-1
siRNA-2
kDa
60
hnRNPK
60
Atf4
60
Tubulin
hnRNPK KD
DMSO
ISRIB
B
Aars
C
Gars
D
Iars
E
Nars
F
Sars
Relative expression
Control
hnRNPK KD
DMSO
ISRIB

Figure 7

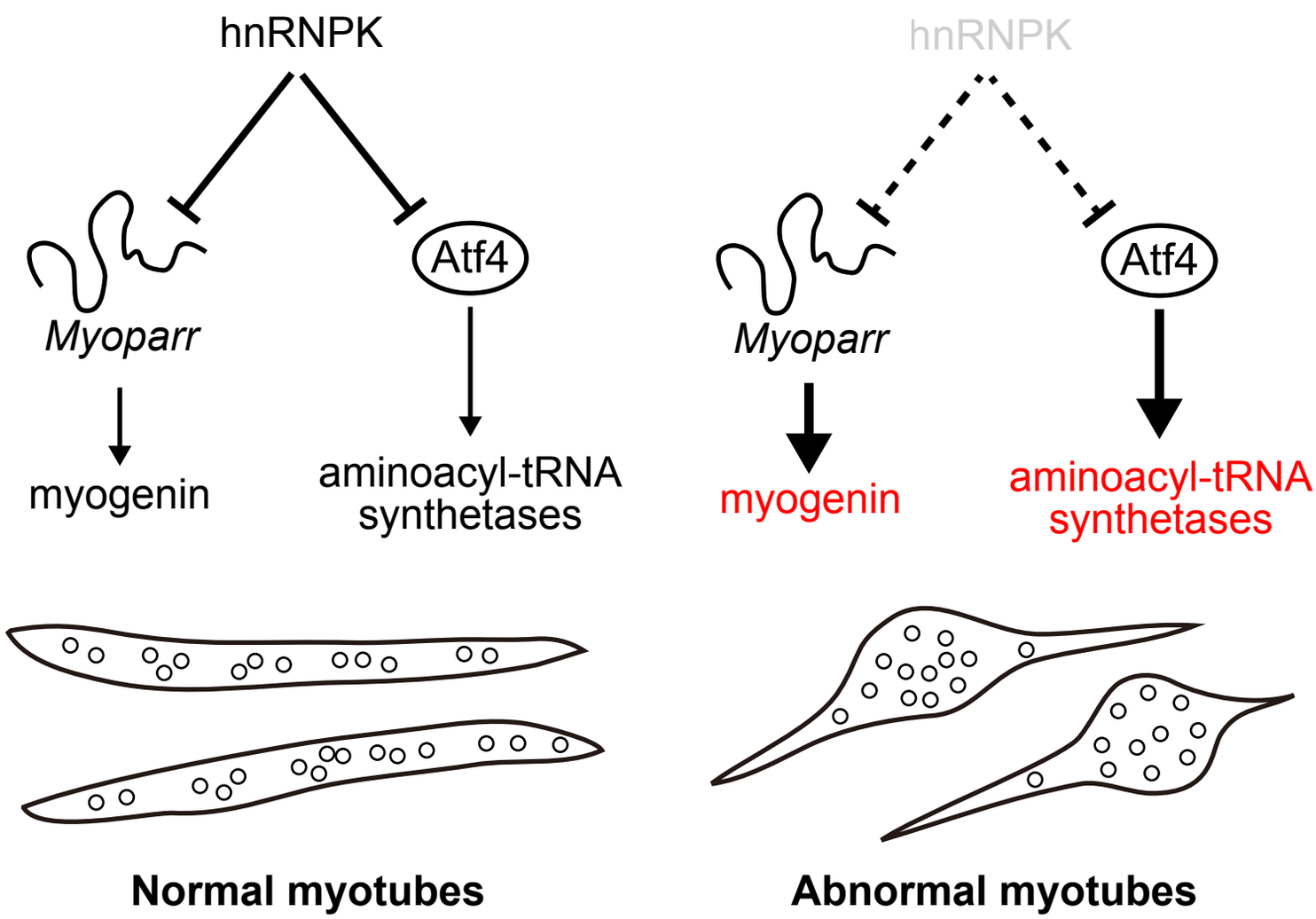
hnRNPK
Myoparr
Atf4
myogenin
aminoacyl-tRNA synthetases
hnRNPK
Myoparr
Atf4
myogenin
aminoacyl-tRNA synthetases
Normal myotubes
Abnormal myotubes

Supplementary Figure 1

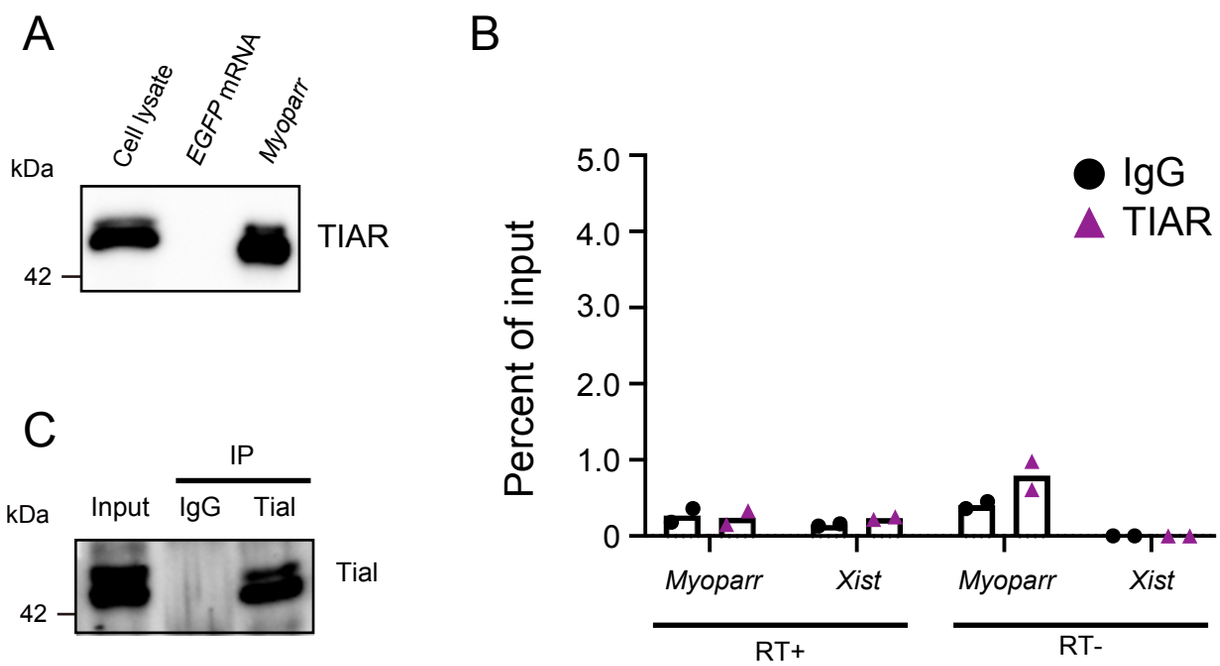

Supplementary Figure 2

A

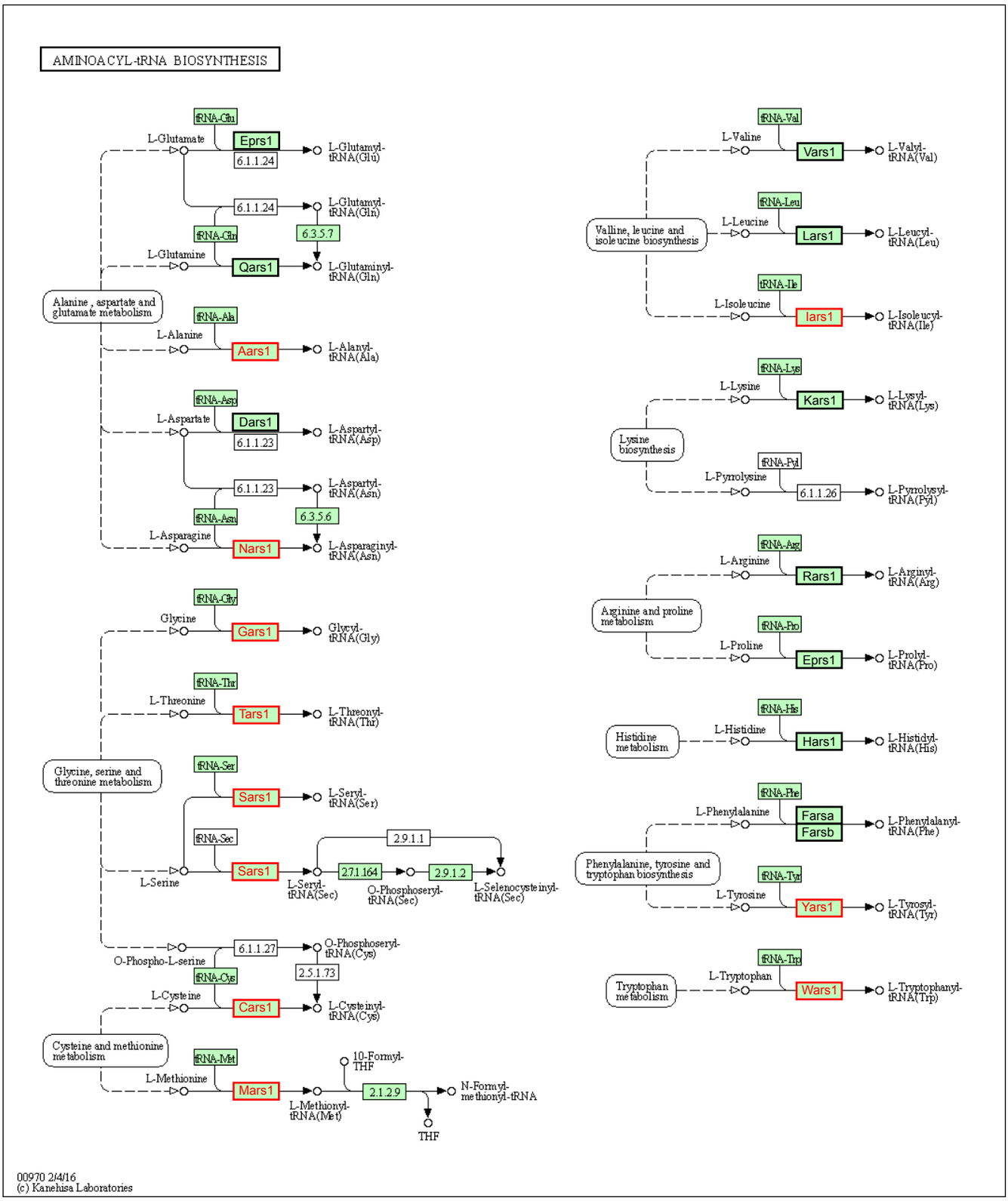

B Cytosolic aminoacyl-tRNA synthetases

Gene Name	Description	log2 Foldchange	padj
Aars (Aars1)	alanyl-tRNA synthetase	1.189688646	6.64E-11
Rars (Rars1)	arginyl-tRNA synthetase	0.717750186	0.000603064
Nars (Nars1)	asparaginyl-tRNA synthetase	1.037402961	1.73E-09
Dars (Dars1)	aspartyl-tRNA synthetase	0.298274648	0.325335115
Cars (Cars1)	cysteinyl-tRNA synthetase	0.872794782	2.21E-05
Qars (Qars1)	glutaminyl-tRNA synthetase	0.081217744	0.864024052
Eprs (Eprs1)	glutamyl-prolyl-tRNA synthetase	0.585228462	0.018216177
Gars (Gars1)	glycyl-tRNA synthetase	1.205275471	3.91E-13
Hars (Hars1)	histidyl-tRNA synthetase	0.413615028	0.200347566
Iars (Iars1)	isoleucine-tRNA synthetase	1.022779598	8.54E-07
Lars (Lars1)	leucyl-tRNA synthetase	0.709821097	0.000114578
Kars (Kars1)	lysyl-tRNA synthetase	0.349181856	0.168606343
Mars (Mars1)	methionine-tRNA synthetase 1	0.900197979	1.01E-05
Farsa	phenylalanyl-tRNA synthetase, alpha subunit	0.200736108	0.620163384
Farsb	phenylalanyl-tRNA synthetase, beta subunit	0.710725176	0.000803764
Sars (Sars1)	seryl-aminoacyl-tRNA synthetase	1.078993838	2.66E-06
Tars (Tars1)	threonyl-tRNA synthetase	0.905000211	8.27E-07
Wars (Wars1)	tryptophanyl-tRNA synthetase	0.878940288	5.01E-06
Yars (Yars1)	tyrosyl-tRNA synthetase	0.772263805	0.000703005
Vars (Vars1)	valyl-tRNA synthetase	0.593311919	0.003371758

C Mitochondrial aminoacyl-tRNA synthetases

Gene Name	Description	log2 Foldchange	padj
Aars2	alanyl-tRNA synthetase 2, mitochondrial	-0.781345711	0.012684624
Rars2	arginyl-tRNA synthetase 2, mitochondrial	0.020716521	0.976825609
Nars2	asparaginyl-tRNA synthetase 2 (mitochondrial)(putative)	0.356286565	0.378947013
Dars2	aspartyl-tRNA synthetase 2 (mitochondrial)	-0.118907946	0.852207722
Cars2	cysteinyl-tRNA synthetase 2 (mitochondrial)(putative)	-0.419664503	0.30297916
Ears2	glutamyl-tRNA synthetase 2, mitochondrial	0.432715891	0.343242224
Hars2	histidyl-tRNA synthetase 2	-0.125988909	0.813766049
Iars2	isoleucine-tRNA synthetase 2, mitochondrial	-0.111305242	0.796505735
Lars2	leucyl-tRNA synthetase, mitochondrial	-0.257452115	0.40655708
Mars2	methionine-tRNA synthetase 2 (mitochondrial)	-0.463741055	0.383638447
Fars2	phenylalanine-tRNA synthetase 2 (mitochondrial)	0.24527022	0.65503804
Pars2	prolyl-tRNA synthetase (mitochondrial)(putative)	0.203237774	0.784806846
Sars2	seryl-aminoacyl-tRNA synthetase 2	-0.782886579	0.039853007
Tars2	threonyl-tRNA synthetase 2, mitochondrial (putative)	0.25526333	0.552363803
Wars2	tryptophanyl tRNA synthetase 2 (mitochondrial)	0.172212967	0.789056335
Yars2	tyrosyl-tRNA synthetase 2 (mitochondrial)	0.078853278	0.90065489
Vars2	valyl-tRNA synthetase 2, mitochondrial	0.188587495	0.706779801

Supplementary Figure 3

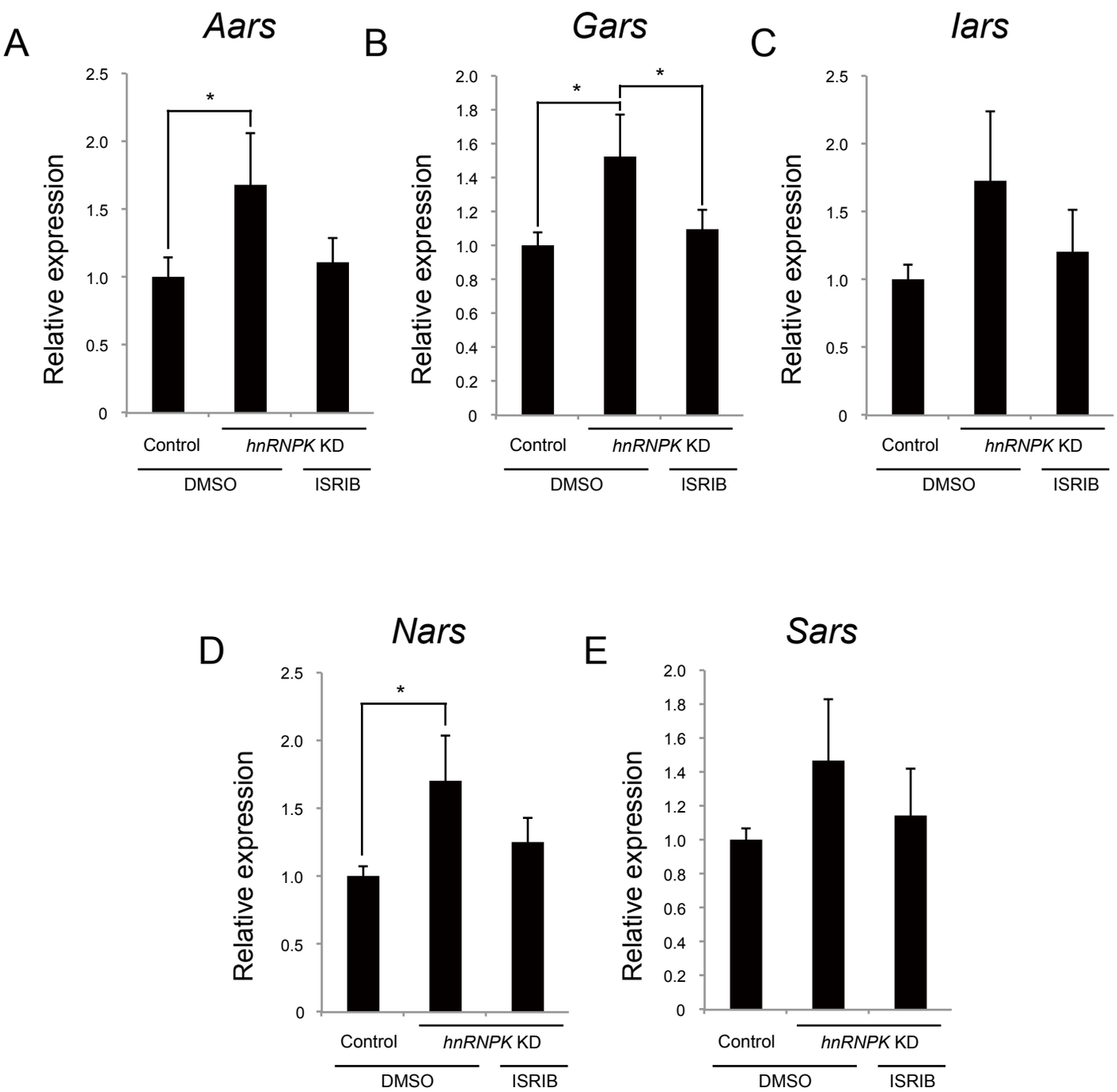

Supplementary Table 1

Primers for real-time PCR analysis		
Target name	Forward	Reverse
myogenin	CAGTACATTGAGCGCCTACAG	GGACCGAACTCCAGTGCAT
Myoparr (1)	GTGCCCTATCGTCCATGGAG	CACTGACTTCACCTGACCCC
Myoparr (2)	GGGCAGGAAGGGAACAAGAA	CCCCAAATCTGGAGTGGTCC
Xist	CCCGCTGCTGAGTGTTTGAT	ATCCAGGCAATCCTTCTTCTTG
Atf4	AAGGAGGAAGACACTCCCTCT	CAGGTGGGTCATAAGGTTTGG
Aars	ATGGATGCCACTTTAACAGCA	TGGGTCGATTGTGTTTAGGAAGA
Gars	GGAGGCAGCACTTTATCCAAG	TCGGAAGCACTCTCCGTTCT
Iars	CCTCCCTTTGCTACTGGACTG	GGTGAGCGTATCTCGTAACGAT
Nars	GAGCTGTATGTATCTGACCGAGA	AAATGGTGGGAAATGGCTCTTT
Sars	CGGGTGGATAAAGGAGGGGA	TGCCCGAAATCTGCATCGTC
hnRNPK	CCGTACAGACTACAATGCCAG	GCCCTCTTCCAAGGTAGGGAT
Rpl26	GGTCTATGCCCATTCGGAAGG	TCGTTCGATGTAGATGACGTACT

siRNA		
Target name	Target Sequence	
Control siRNA	-	Stealth RNAi siRNA Negative Control, Med GC (Thermo Fisher Scientific)
Myoparr siRNA	GATGGACCCTGTCTGATGCTCTTAA	Thermo Fisher Scientific
hnRNPK siRNA-1	TCCCAAAGATTTGGCTGGATCTATT	MSS205172 (Thermo Fisher Scientific)
hnRNPK siRNA-2	GGAAGTGACTTTGATTGCGAGTTGA	MSS205173 (Thermo Fisher Scientific)